THE ROYAL SOCIETY
PUBLISHING

Alfvén Pulse Driven Spicule-like Jets in the Presence of Thermal Conduction and Ion-Neutral Collision in Two-Fluid Regime

A. K. Srivastava[1], Anshika Singh[1], Balveer Singh[2], K. Murawski[3], T.V. Zaqarashvili[4], D. Yuan[5], E. Scullion[6], Sudheer K. Mishra[7], B. N. Dwivedi[8]

[1]Department of Physics, Indian Institute of Technology (BHU), Varanasi 221005, India; [2]Aryabhatta Research Institute of Observational Sciences (ARIES), Manora peak, Nainital 263001, India; [3]Institute of Physics, University of Maria Curie-Sklodowska, Pl. M. Curie-Sklodowskiej, 20-0531 Lublin, Poland; [4]Institut of Physics, IGAM, University of Graz, Universitätsplatz 5, 8010, Graz, Austria; [5]Shenzhen Key Laboratory of Numerical Prediction for Space Storm, Institute of Space Science and Applied Technology, Harbin Institute of Technology, Shenzhen, Guangdong 518055, China; [6]Northumbria University, NE1 8ST Newcastle upon Tyne, UK; [7]Astronomical Observatory, Kyoto University, Sakyo, Kyoto 606-8502, Japan; [8]Rajiv Gandhi Institute of Petroleum Technology, Jais Amethi 229304, India

We present the formation of quasi-periodic cool spicule-like jets in the solar atmosphere using 2.5-D numerical simulation in two-fluid regime (ions+neutrals) under the presence of thermal conduction and ion-neutral collision. The non-linear, impulsive Alfvénic perturbations at the top of the photosphere trigger field aligned magnetoacoustic perturbations due to ponderomotive force. The transport of energy from Alfvén pulse to such vertical velocity perturbations due to ponderomotive force is considered as an initial trigger mechanism. Thereafter, these velocity perturbations steepen into the shocks followed by quasi-periodic rise and fall of the cool jets transporting mass in the overlying corona.

1. Introduction

The complex magnetic field structuring and highly dynamic nature of the Sun's chromosphere permit the genesis of numerous high speed jet-like plasma ejecta at different time and spatial scales [1–8]. These cool spicule-like jets are significant dynamical plasma processes that may be accompanied with various types of waves, oscillations, instabilities etc in the Sun's atmosphere [5,6,9–13]. Such confined and cool jet like features may be one of the possible sources to carry energy and mass from the inner layers (i.e., photosphere, chromosphere) of the solar atmosphere into its upper layers (i.e, transition region, and corona). These jet-like phenomena evoked the scientific research since long keeping the view of the advent of many space-borne and ground-based, high-resolution solar observations, as well as theoretical/numerical modelling [1,2,6,14–21]. These jets may also have impulsive origin, and they could exhibit quasi-periodic upward and downward plasma motions along their spine in the localized solar atmosphere. There are several observational and theoretical results available, which frequently describe their origin, evolution, physical properties and associated plasma processes [6–8,14,22]. However, their exact triggering mechanisms are still unclear, thereby detailed investigation is always an essential requirement using observations with high resolution observations as well as extensive numerical modelling.

Recently, multi-wavelength and high spatio-temporal resolution observations taken from ground and space based observatories reveal the triggering and evolution of small-scale cool and thin spicule-like jets. These jets can be observed for example in H_{α}, Na D3, Ca II spectra of the solar chromosphere, which reveal their double-thread structures, detailed morphology, kinematics, and property of quasi-periodical rise and fall [1,2,6,8,14–17,21,22]. Although many of them allude to the similar basic structure and plasma configuration, these cool jets have a variety of nomenclature and morphology depending on where and how they are observed. The family of cool chromospheric jets show-up distinct morphological, evolutionary, and kinematical properties (e.g., type I spicule, type II spicule, network jets, macrospicules, fibrils, mottles, swirls etc). Spicules are mainly seen on the solar limb propagating with the speed of about 25 km s^{-1}, which is greater than supersonic speed in the chromosphere. These cool jets trace the magnetic field lines. They are referred to type I spicules. There are plenty of studies also considering such ejecta observed on the solar disk in form of RRE/RBEs, fibrils, etc. The type I spicules have a maximum height of 7-10 Mm, typical lifetime of 5-15 min, and lateral width of 500 km. [23]. On the other hand, the cool jets propagate with a typical high speed of $\approx$ 50-100 km s^{-1}, attain their maximum height of $\approx$ 4 Mm, referred as type II spicule. Its width is $\approx$ 200 km, and typical lifetime $\approx$ 10-15 sec. These spicules are also seen rapidly fading in chromospheric absorption lines [2,16]. This phenomenon appears due to the fact that the jet's cool plasma material quickly expand or fade away by the heating process [24,25]. The life-time of the Type II spicule also depends on the observables as seen in Ca II emissions from the solar chromosphere. They disappear, but their life-time is longer at the lines formed higher up in the solar atmosphere, e.g., C II or Si IV [24]. Some of type II spicules are found in coronal holes but especially in plage regions exhibiting their maximum height $\approx$ 5 Mm.The detailed physical properties of type-I and II spicules are described in [26].

In addition, the large-scale similar spicule-like jets are also commonly observed in the solar atmosphere. They are termed as macrospicules. They have impulsive origin and attain a maximum height of 7-70 Mm. Their typical lifetime is about 3-15 min, and vertical flow rate is $\approx$10-150 km s^{-1} [27–31]. These comparatively larger spicules may be observed in the polar region of the coronal holes. More-recently, the high spatio-temporal (SJI) and spectral resolution observations taken from Interface Region Imaging Spectrograph (IRIS) reveal the cool and thin jets mainly rooted in the magnetic networks below the corona with a typical apparent speed $\approx$80-250 km s^{-1} , and termed as network jets [2,32,33]. Their maximum height is $\approx$ 10 Mm and typical lifespan is 20-80 s. The quiet-Sun network jets may also rotate with an apparent velocity of $\approx$50 km s^{-1} [32,34]. In addition , the larger cool jets may also exhibit the tendency of helical/rotatory motion, and their spire can acquire magnetic twists [34–36]. In particular, the large-scale cool

plasma jets and surges are usually linked with flux emergence/cancellation. The cool counterpart of the surges are observed in the blue/red shifted absorption lines in H-α observations and Ca II H & K lines [37–40]. These surges may possess initiation velocity of about 50 km s^{-1}, which could increase upto a maximum of 100-300 km s^{-1} [37]. Such cool jets may attain a height of 10–200 Mm or greater [37,41]. The lifetime of surges is calculated on average about 30 minutes, while they may periodically rise and fall with a period of an hour or longer [37,41,42].

Various theoretical and extensive numerical models have been performed in recent years to understand the physical features, triggering/formation mechanism and associated plasma processes of such cool jets. The evolution of these cool jets may also be most likely associated with small-scale magnetic reconnection in the solar photosphere/chromosphere. This physical process may result in an energetic explosion in the solar chromosphere/photosphere, which may indirectly affect the localized magneto-plasma region further resulting in the triggering of cool jet-like motions moving upward through the magnetic field lines [43]. The evolution and formation of the jets are determined by the height and the magnitudes of the reconnection whether it is occurred near the photosphere or in the upper chromosphere. When the reconnection occurs near the solar photosphere, the plasma outflows collides with the high plasma beta region and moves along the magnetic field lines. This dynamics eventually triggers a slow-mode wave further steepens as a strong slow shock while propagating upward in the solar atmosphere. When this shock passes through the transition region, it lifts cool plasma jets. Eventually when magnetic reconnection occurs in the upper part of the solar chromosphere, the cool plasma is accelerated in the form of jets because of the collective effect of Lorentz force and the transverse whip-like motions of the magnetic field lines [25,43–46]. Another classical scenario of the formation of such cool jets is the onset of energy deposition by pressure pulses or velocity pulses at chromospheric/photospheric heights. As a result, eventually an evolution of the magnetoacoustic shock enables the motion of the plasma in form of the cool jets. In such models, the applied pulses act as a driver and create localized heating or transfer of momentum resulting into shocks and generating the jet-like features [1,4,6,14,22,44,47,48]. The process generally proposed as the agents causing the formation of cool spicular jets and other chromospheric cool plasma ejecta (e.g., cool jets, network jets, macrospicules, spicules, swirls etc) is the shock-generated model [1,4,6,7,14,27,44,47,49]. Hansteen et al [14] reported the formation of cool jet-like plasma ejections (e.g., dynamic fibrils, mottles etc) from the active regions driven by slow-mode upward propagating magnetoacoustic shocks. The formation of these shocks is caused by waves motion triggered by the random convective flows and evolution of the global p-mode oscillations at the photosphere. The Alfvén waves/pulses are also put forward as a trigger of the spicular jets in the chromosphere [6,50,51]. Hollweg [50] proposed a MHD model for the formation and evolution of spicule-like cool jets using an Alfvén pulse of the magnitude of 1 km s^{-1} at the photosphere. Recently, Singh B et al. [6] delineated the comprehensive physical scenario about the origin and motions of the cool spicular jets in the ideal, single fluid MHD by implementing large-amplitude Alfvén pulse at the chromospheric height. These jets show quasi-periodic rise and fall in the model solar atmosphere and describe the physical manifestation of spicules. There are several single fluid MHD model in ideal and non-ideal regime, that clearly depicts the generation of cool spicular jets [52,53].

Additionally, two fluid numerical models understand the multi-fluid physical effects and their roles as compared to single fluid models. Therefore, two fluid models are one of the more convincing methods providing the new insight of the triggering and physical properties of such spicule-like jets. The partially ionized solar chromosphere contains ions, electrons and neutrals. Many models of the solar chromosphere, therefore, include non-ideal factors like conduction, radiative cooling, and dissipation predominantly caused by the ion-neutral collisions, providing crucial information regarding the heating and plasma dynamics in the chromosphere [54–56]. James et al. [57] have described the generation of spicules caused by the dissipation of high-frequency Alfvén waves/pulse invoking the physics of ion-neutral collision damping in axisymmetric and initially untwisted flux tubes by performing 1.5-D simulation. The dissipation

of waves attributed by ion-neutral collisions and thermal conduction, in general take place to deposit the additional energy in the solar chromosphere that subsequently takes into account the evolution of spicular cool jets [58–62].

In this work, we have carried out a 2.5-D numerical simulation in two-fluid regime. In the presence of ions and neutrals along with ion-neutral collisions and thermal conduction we provide a perspective of the triggering of cool spicule-like jets triggered initially by the implementation of Alfvén pulse at the solar chromosphere. We impose a non-linear, impulsive Alfvén pulse in the solar chromosphere to drive the cool spicular jets in the realistic temperature and gravitationally stratified model of the vetically structured solar atmosphere. Previously, [6] proposed a model of the spicule-like cool jets in ideal, single-fluid MHD by implementation of randomly generated multiple Alfvén pulses of magnitudes 50-90 km s^{-1} in the solar chromosphere . In the present work, we revisit this previously proposed case of ideal MHD, and here we perform a 2.5-D numerical model for the evolution and triggering of cool jets in two-fluid (ions & neutrals) regime of the chromospheric plasma taking into account thermal conduction and ion-neutral collision using JOANNA code. We find that the existence of ion-neutral collisions and thermal conduction influence the evolution and kinematics of such spicular jets triggered initially by non-linear Alfvén pulses in the chromosphere. These physical candidates are required for the formation of such spicular cool jets in the solar chromosphere. In this paper, we investigate the triggering mechanism and evolution of these cool jets which closely match with the observations. This paper is put in the order as follows. The basic two-fluid model and initial setup of the solar atmosphere are presented in Section 2. The numerical simulation and its results are described in Section 3. The discussion and conclusions of this work are presented in Section 4.

2. Model and initial configuration

(a) The Two-Fluid Model

In this model, we consider the two-fluid system consisting of ions and neutrals along with ions-neutral collisions. We do not consider the consequences of recombination and ionisation of ions and neutrals. We also take into account the thermal conduction which contributes in the formation/dynamics of the cool jets. The governing equations of two-fluid system in the solar magnetized plasma are given as follows [56,58,61,63–70]:

$$\frac{\partial \varrho_i}{\partial t} + \nabla \cdot (\varrho_i \mathbf{V}_i) = 0, \tag{2.1}$$

$$\frac{\partial \varrho_n}{\partial t} + \nabla \cdot (\varrho_n \mathbf{V}_n) = 0, \tag{2.2}$$

$$\varrho_i \left(\frac{\partial \mathbf{V}_i}{\partial t} + (\mathbf{V}_i \cdot \nabla)\mathbf{V}_i \right) = -\nabla p_i + \frac{1}{\mu}(\nabla \times \mathbf{B}) \times \mathbf{B} + \varrho_i \mathbf{g} \\ - \alpha_c(\mathbf{V}_i - \mathbf{V}_n), \tag{2.3}$$

$$\varrho_n \left(\frac{\partial \mathbf{V}_n}{\partial t} + (\mathbf{V}_n \cdot \nabla)\mathbf{V}_i \right) = -\nabla p_n + \varrho_n \mathbf{g} \\ + \alpha_c(\mathbf{V}_i - \mathbf{V}_n), \tag{2.4}$$

$$\frac{\partial \mathbf{B}}{\partial t} = \nabla \times (\mathbf{V_i} \times \mathbf{B}), \qquad \nabla \cdot \mathbf{B} = 0. \tag{2.5}$$

$$\frac{\partial E_i}{\partial t} + \nabla \cdot \left[\left(E_i + p_i + \frac{\mathbf{B}^2}{2\mu} \right) \mathbf{V}_i - \frac{\mathbf{B}}{\mu}(\mathbf{V}_i \cdot \mathbf{B}) \right] = \\ Q_i + (\varrho_i \mathbf{g} + \alpha_c(\mathbf{V}_n - \mathbf{V}_i)) \cdot \mathbf{V}_i + \nabla \cdot \mathbf{q_i}, \tag{2.6}$$

$$\frac{\partial E_{\mathrm{n}}}{\partial t} + \nabla \cdot ((E_{\mathrm{n}} + p_{\mathrm{n}})\mathbf{V}_{\mathrm{n}}) = Q_{\mathrm{n}} + (\varrho_{\mathrm{n}}\mathbf{g} - \alpha_{\mathrm{c}}(\mathbf{V}_{\mathrm{n}} - \mathbf{V}_{\mathrm{i}})) \cdot \mathbf{V}_{\mathrm{n}} + \nabla \cdot \mathbf{q_n} \,, \tag{2.7}$$

Here

$$E_{\mathrm{i}} = \frac{p_{\mathrm{i}}}{\gamma - 1} + \frac{1}{2}\varrho_{\mathrm{i}}|\mathbf{V}_{\mathrm{i}}|^2 + \frac{|\mathbf{B}|^2}{2\mu}, \tag{2.8}$$

and

$$E_{\mathrm{n}} = \frac{p_{\mathrm{n}}}{\gamma - 1} + \frac{1}{2}\varrho_n|\mathbf{V}_{\mathrm{n}}|^2 \,, \tag{2.9}$$

Here, the subscripts 'i' and 'n' depict respectively the components of ions and neutrals. The symbols $\varrho_{\mathrm{i,n}}$ represent the mass densities, $p_{\mathrm{i,n}}$ thermal pressures, and $V_{\mathrm{i,n}}$ is the plasma velocity. B denotes the magnetic field. The constant μ appear for the magnetic permeability. We consider the specific heats ratio represented by γ, which is equal to 5/3. The g=[0,-g,0] depicts the acceleration due to gravity at the Sun. We fix the value of 'g' equal to 274.78 m s^{-2} that is an average value at the solar surface i.e., photosphere. The Hall term electron pressure has been neglected in ideal magnetic induction equation (Eq. 2.5), and the diffusion is numerical. The E_i and E_n expressed as total energy densities. The coefficient α_c denotes the ion-neutral collisions expressed as follows [56,71,72]:

$$\alpha_{\mathrm{c}} = \frac{4}{3}\frac{\sigma_{\mathrm{in}}\,\varrho_{\mathrm{i}}\,\varrho_{\mathrm{n}}}{m_H(\mu_{\mathrm{i}} + \mu_{\mathrm{n}})}\sqrt{\frac{8k_B}{\pi m_H}\left(\frac{T_{\mathrm{i}}}{\mu_{\mathrm{i}}} + \frac{T_{\mathrm{n}}}{\mu_{\mathrm{n}}}\right)} \,. \tag{2.10}$$

Here, m_H represents the hydrogen mass, k_B is the Boltzmann's constant, the symbols $\mu_{i,n}$ represent the mean mass of the ions and neutrals, respectively. We fix the value of $\mu_i = 0.58$ for ions+electrons and $\mu_n = 1.21$ for neutrals from the given solar abundance [56]. The symbols $T_{i,n}$ denote the temperature of ions and neutrals, respectively. The symbol σ_{in} represents the cross-section of ion-neutral collision as a quantum value equal to 1.4×10^{-15} m^2 for momentum exchange among the particles [56,73].

The additional terms in the energy equations 'Q_i' and 'Q_n' represent the frictional interaction between particles resulting generates the additional heat, which are expressed as:

$$Q_{\mathrm{i}} = \alpha_c \left[\frac{1}{2}|\mathbf{V}_{\mathrm{i}} - \mathbf{V}_{\mathrm{n}}|^2 - \frac{3}{2}\frac{k_B}{m_{\mathrm{H}}(\mu_{\mathrm{i}} + \mu_{\mathrm{n}})}(T_{\mathrm{i}} - T_{\mathrm{n}})\right] \,, \tag{2.11}$$

$$Q_{\mathrm{n}} = \alpha_c \left[\frac{1}{2}|\mathbf{V}_{\mathrm{i}} - \mathbf{V}_{\mathrm{n}}|^2 - \frac{3}{2}\frac{k_B}{m_{\mathrm{H}}(\mu_{\mathrm{i}} + \mu_{\mathrm{n}})}(T_{\mathrm{n}} - T_{\mathrm{i}})\right] \,, \tag{2.12}$$

In this model, the divergence of the embedded magnetic field lines (B) was kept small. Here, we do not take into account some non-ideal dissipative effects such as viscosity, resistivity, plasma cooling and/or heating, magnetic diffusivity etc. However, we implement in the model the effect of thermal conduction by figuring out the heat flux vector ($q_{i,n}$). In case of neutrals, thermal conduction is isotropic which is expressed as follows:

$$\mathbf{q}_{\mathrm{n}} = \kappa_{\mathrm{n}}\nabla T_{\mathrm{n}} \,. \tag{2.13}$$

Here, κ_{n} depicts the coefficient of thermal conduction in case of neutrals which is expressed as [70,74]

$$\kappa_{\mathrm{n}} = \frac{29.6\,T_{\mathrm{n}}}{1 + \sqrt{7.6 \cdot 10^5\,\mathrm{K}/T_{\mathrm{n}}}}\frac{\mu_{\mathrm{n}}m_H}{k_{\mathrm{B}}} \,, \tag{2.14}$$

where k_{B} is 1.3807×10^{-16} cm^2 g s^{-2} K^{-1}.

Thermal conduction for the ions, is highly anisotropic that permits the flow of heat through the length of magnetic field lines. However, the heat flux vector across the length of the magnetic field lines is negligibly small. The expression for the heat flux (q_i) is expressed as
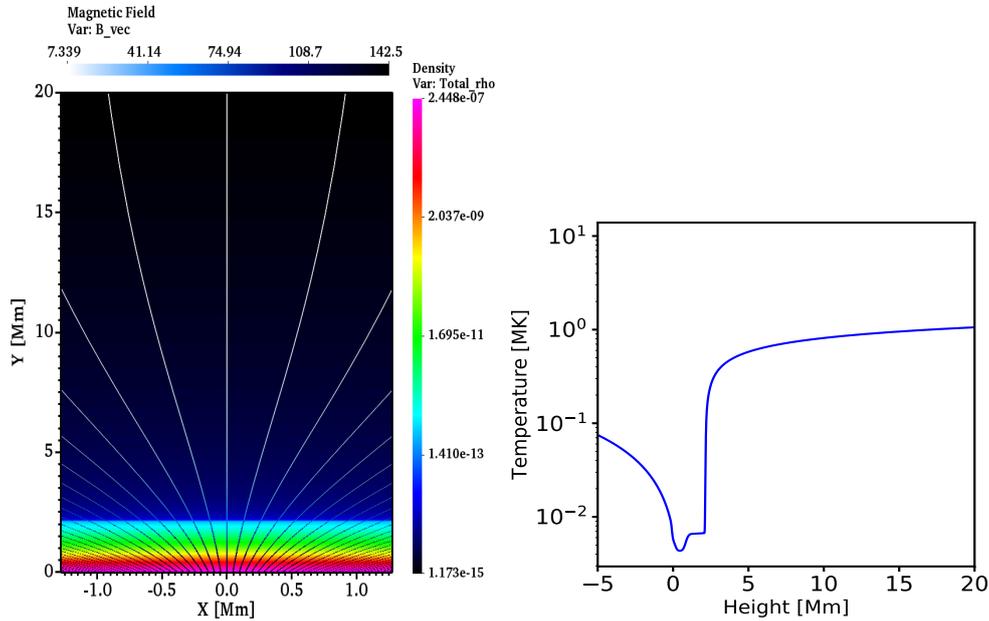
Figure 1. The left image displays smoothly curved and expanding magnetic field lines permeating the gravitionally stratified solar atmosphere maintained initially at an equilibrium from the solar photosphere upto the inner corona. The density and magnetic field strength in colorbar are given in g cm^{-3} and Gauss respectively. The right panel shows the temperature variation as a function of height in this vertically (or longitudinally) structured localized solar atmosphere as theorized by Avrett & Loeser [77].

$$\mathbf{q}_{\mathrm{i}} = \kappa_{\parallel} \mathbf{b} \nabla (\mathbf{b} \cdot T_{\mathrm{i}}) \,, \tag{2.15}$$

where $b = B/B$ depicts the unit vector aligning in the direction of the magnetic field. The coefficient of thermal conduction $\kappa_{\parallel}$ is expressed as [70,75]:

$$\kappa_{\parallel} \approx 4.6 \cdot 10^{13} \left(\frac{T_{\mathrm{e}}}{10^8 \, \mathrm{K}} \right)^{5/2} \frac{40}{\Lambda_c} \quad [\mathrm{erg \, s^{-1} \, cm^{-1} \, K^{-1}}] \tag{2.16}$$

Here, Λ_c denotes the quantum Coulomb logarithm which is expressed as [70,76]

$$\Lambda_c \approx 30.9 - \log \frac{n_{\mathrm{e}}^{1/2}}{T_{\mathrm{e}} k_{\mathrm{B}}^*} \,. \tag{2.17}$$

Here, the Boltzmann constant k_{B}^* is expressed in eV K^{-1}. The symbol n_e represents the electron particle number density, while T_e is the electron temperature as expressed in eV.

(b) Equilibrium Configurations of the Model Solar Atmosphere

Initially, the considered model atmosphere extending from the solar photosphere to the inner corona is in equilibrium state. As the average flow at the transition region is estimated to be of the order of about 3 km s^{-1} (e.g. Avrett & Loeser [77]), initially (at t=0 s) we set the quasi-static (V_i=V_n=0) atmosphere. In addition, the Lorentz force affects only the ions while neutrals are obviously remain unaffected. Therefore, the equations 2.3 and 2.4 can be written as follows:
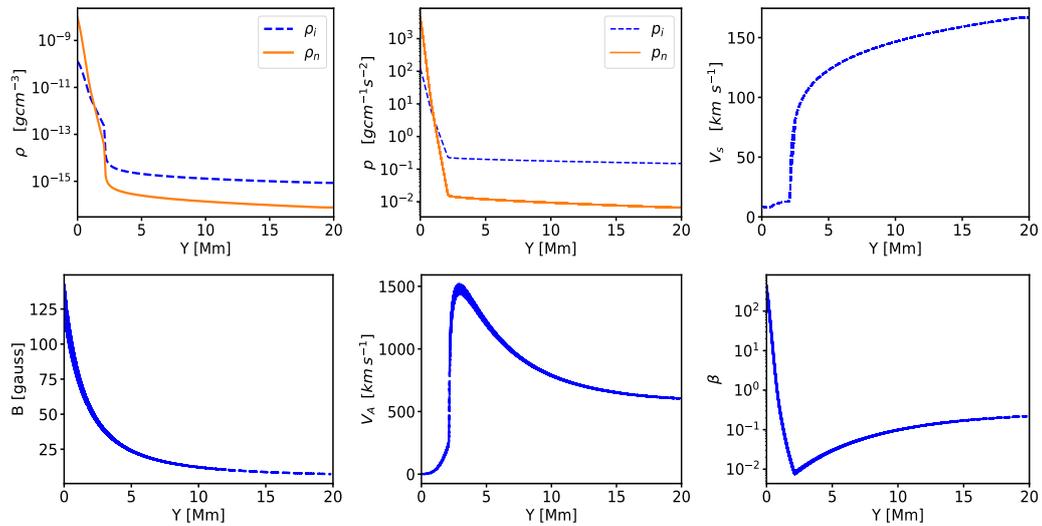
Figure 2. The physical background parameters vs height. Top left panel shows respectively the mass density for ions (blue-curve) and neutrals (magenta-curve). The top-middle panel demonstrates respectively the plasma pressure for ions (blue-curve) and neutrals (magenta-curve). The sound speed (top-right), magnetic field (bottom-left), Alfvén speed (bottom-middle), and plasma beta (bottom-right) are also displayed.

$$0 = -\nabla p_i + \rho_i \boldsymbol{g} + \frac{1}{\mu}(\nabla \times \boldsymbol{B}) \times \boldsymbol{B} \tag{2.18}$$

and

$$0 = -\nabla p_n + \rho_n \boldsymbol{g} \tag{2.19}$$

We take into account an appropriate magnetised solar atmosphere that constitutes the region between convection zone (-3.0 Mm) and corona (20 Mm). The model solar atmosphere follows the hydrostatic equilibrium for ions initially immersed in the force free and current free magnetic field given as

$$(\nabla \times \mathbf{B}) \times \mathbf{B} = 0, \qquad \nabla \times \mathbf{B} = 0. \tag{2.20}$$

The horizontal ($\boldsymbol{B}_x$) component, vertical ($\boldsymbol{B}_y$) component, and transversal ($\boldsymbol{B}_z$) component of the equilibrium magnetic field are expressed as per the B.C. Low model: [6,78]

$$B_x(x,y) = \frac{-2S(x-a)(y-b)}{((x-a)^2 + (y-b)^2)^2}, \tag{2.21}$$

$$B_y(x,y) = \frac{2S(x-a)^2 - S((x-a)^2 + (y-b)^2)}{((x-a)^2 + (y-b)^2)^2} + B_v, \tag{2.22}$$

$$B_z(x,y) = 0. \tag{2.23}$$

Here, the symbol 'S' denotes the magnitude of the magnetic pole. The variables 'a' and 'b' respectively represent the horizontal and vertical location of this singular magnetic pole. We choose its magnitude as S $\simeq$1240 Gauss in the sub-photospheric layer, i.e., convection zone, at the position of (a,b)=(0,-3.0) Mm. We also fix the additional magnetic field B$_v$=5 Gauss in the solar corona (i.e., y$_{ref}$=50 Mm) which forms quiet-Sun atmosphere with sufficiently strong magnetic field. The magnetic line of forces come out from the chosen pole in the convection zone and fan-out through the photosphere in the inner corona as displayed in the left-panel of Fig. 1. The strength (or magnitude) of the magnetic field falls-off with height in corona according to Eqs. 2.17, 2.18 and 2.19.

The modelled solar atmosphere is also maintained by the force-free condition in the background. Therefore, the gravity force equalises the pressure gradient force, making the medium approximately force-free. It is possible to express it as follows [56,79]:

$$p_{i,n} = p_{0i,n} \exp \left(- \int_{y_{ref}}^{y} \frac{dy'}{\Lambda(y')} \right),$$ (2.24)

$$\varrho_{i,n} = \frac{p_{i,n}}{g\Lambda(y)},$$ (2.25)

where,

$$\Lambda(y) = \frac{k_B T_{i,n}}{mg},$$ (2.26)

$$p_{i,n} = \frac{\rho_{i,n} T_{i,n} k_B}{m_H \mu_{i,n}}.$$ (2.27)

where, $p_{0i,n}$ representing the thermal pressure of ions as well as neutrals at the given reference point (i.e., y_{ref} = 50 Mm). We fix the value of $p_{0i} = 10^{-1}$ dyn cm^{-2} and $p_{0n} = 3 \times 10^{-3}$ dyn cm^{-2} at the y_{ref}=50 Mm in the inner corona. Initially (at t=0), we assume that $T_i(y)=T_n(y)$ but later on they are allowed to evolve according to the two-fluid model.

Initially, we adopt the realistic temperature profile which is theorized by Avrett & Loeser [77], using various line profiles recorded at multiple heights (regions) of the solar atmosphere (see right panel of Fig. 1). The mosaic of Fig. 2 shows the density (top left), thermal pressure (top middle), sound speed (top right), magnetic field (bottom left), Alfvén speed (bottom middle), and plasma beta (bottom right) as a function of height in the gravitationally stratified and magnetized solar atmosphere. It depicts the longitudinal (or vertical) structuring of the model soalar atmosphere. The mass density of the plasma gas and its thermal pressure for ions (p_i) and neutrals (p_n) at different heights, are estimated using equations Eqs. 2.20-2.23. The detailed descriptions as given above demonstrate that we employ a realistic, magnetically and gravitationally stratified model of the solar atmosphere to understand the generation of cool spicule-like jets.

(c) Numerical Methods

We numerically solve the complete set of two-fluid equations within JOANNA code [56,61] by carrying out the implementation of initial and boundary conditions. To assure stability and accuracy in the present simulation, we fix the Courant–Friedrichs–Lewy (CFL) number as 0.3 and use 2nd-order Runge-Kutta (RK2) numerical technique for time stepping because it is a self-starting method for solving the differential equations. The source terms such as ion-neutral drag force and thermal conduction are stiff and therefore they require an explicit treatment [56,61]. Furthermore, we have employed Harten-Lax-van Leer discontinuities (HLLD) as a Riemann solution to improve shock stability and low-speed flow accuracy. We set the model solar atmosphere of 2.56 Mm ($-1.28 \leq x \leq 1.28$) Mm in x, and 20 Mm in y ($0 \leq y \leq 20$) Mm. We hold the static uniform grid from 0 Mm up to 5.12 Mm in the y-direction, and fix the stretched grid above y=5.12 Mm up to y=20 Mm. The spatial resolution in the zone of uniform grid is 10 km. In the upper part of the model solar atmosphere, the proper stretched grid has been employed which acts like a sponge, effectively soaking up the incoming signals and minimizing the amount of reflection from the top boundary. As a result, there is no substantial reflected signals are seen in the system, particularly in the top zone of the numerical domain. The majority of the energy exchange from Alfvén pulse occurs in the chromosphere-TR-inner corona below y=5.0 Mm, and cool jets propagate in that particular region only. We impose all four boundaries on the simulation box to ensure that all the boundaries continue to preserve the equilibrium in the physical parameters. More specifically, at the bottom and top boundaries of the numerical domain, we hold fixed all plasma quantities to their equilibrium values and at the side boundaries we use open boundary conditions. We found that top and bottom boundaries minimize numerically

induced reflections of the incoming signal, and the open side boundaries allow the signal to leave the simulation box. It is the appropriate way to have boundaries that function relatively well when gravity is present in the system. We run the numerical simulations for 1000 s utilizing multiple passage interface (MPI) and save the output files every 5 s.

(d) Perturbations

At an initial time of the present two-fluid simulation i.e., at t= 0 s, we impose the transverse velocity pulse V_z in ions and neutrals both, which mimic the Alfvén pulse as given by the following eq. [6]:

$$V_z = A_v \times exp\left(-\frac{(x-x_0)^2 + (y-y_0)^2}{w^2}\right). \tag{2.28}$$

In above Eq., A_v appears for the amplitude of the applied driver. The symbols x_0 and y_0 are respectively the horizontal and vertical positions of the pulse, while 'w' is its width, which is taken as 50 km. We impose the amplitude of Alfvén pulse (A_v)= 150 km s^{-1} at (x_0, y_0) = (0, 1.5) Mm, which corresponds to non-linear and impulsive in nature. The applied amplitude of the Alfvén pulse is strong enough to trigger cool jets via energy exchange through ponderomotive force. It is chosen in the light of previously existing knowledge that non-linear, large amplitude transversal perturbations and accompanying Alfvén wave propagation have already been observed in the localized solar atmosphere [80]. In 2.5-D regime, we implement the transverse Alfvén pulse by applying velocity pulse in the ignorable horizontal z-direction. The spicule-like structures in the chromosphere were observed to carry the large amplitude Alfvén motions on their spine [80]. Such impulsive motions can give a sling-shot transverse pulse (an Alfvénic whip-like motion) or periodic wave-like motions to the flux tubes, leading to similar physical conditions as those modeled in the present paper. However, on the contrary, some other observations do not reveal such high, non-linear, and impulsive velocity perturbations in waves, e.g., by measuring line widths, for instance [3,81]. The present model has extreme amplitudes larger than the above mentioned observations and future work should address this. So, we conclude that the driver that we choose in the present work is an episodic driver which can launch spicules or other cool jets through impulsive processes occurring in the localized solar chromosphere. In the non-ideal and two fluid plasma where ion neutral collision and thermal conduction were at the work, the high amplitude of the pulse in our case has only generated the ponderomotive force in the chromosphere, and triggered the field aligned perturbations. Therefore, the presented physical model should be considered as an impulsive and episodic origin of cool jets where reconnection generated velocity perturbations are likely formed in the localized lower solar atmosphere.

3. Results

We have employed the transverse pulse *akin* of Alfvén pulse in both ions and neutrals velocities in the lower solar chromosphere. The non-linear Alfvén pulse is concentrated in a relatively small spatial region of the chromosphere initially, i.e., 50 km. Initially, the applied magnitude of the pulse is high enough (150 km s^{-1}) to non-linearly coupled with the field-aligned magnetoacoustic perturbations to further drive cool jets along the field lines (Fig. 3). The amplitude of the applied pulse conduct itself as an initial driver in the formation of these cool jets.

Fig. 3 shows the evolution of cool jets in both ρ_i and ρ_n. The velocity vectors (red arrows) overlaid on density maps in Fig. 3 depict the velocity of upward moving and downflowing species in the localised model solar atmosphere. The ionization fraction, $\rho_i(y)/(\rho_i(y) + \rho_n(y))$, varies in time. It is higher in the corona. It is also suggestive that due to Lorentz force magnetic field pushes ions and as they are weakly coupled in the chromosphere with neutrals, later became even less abundant there. Although this much ion-neutral coupling is sufficient for ions which are driven by B to drag neutrals and create jets seen both in ρ_i and ρ_n or in their temperatures.
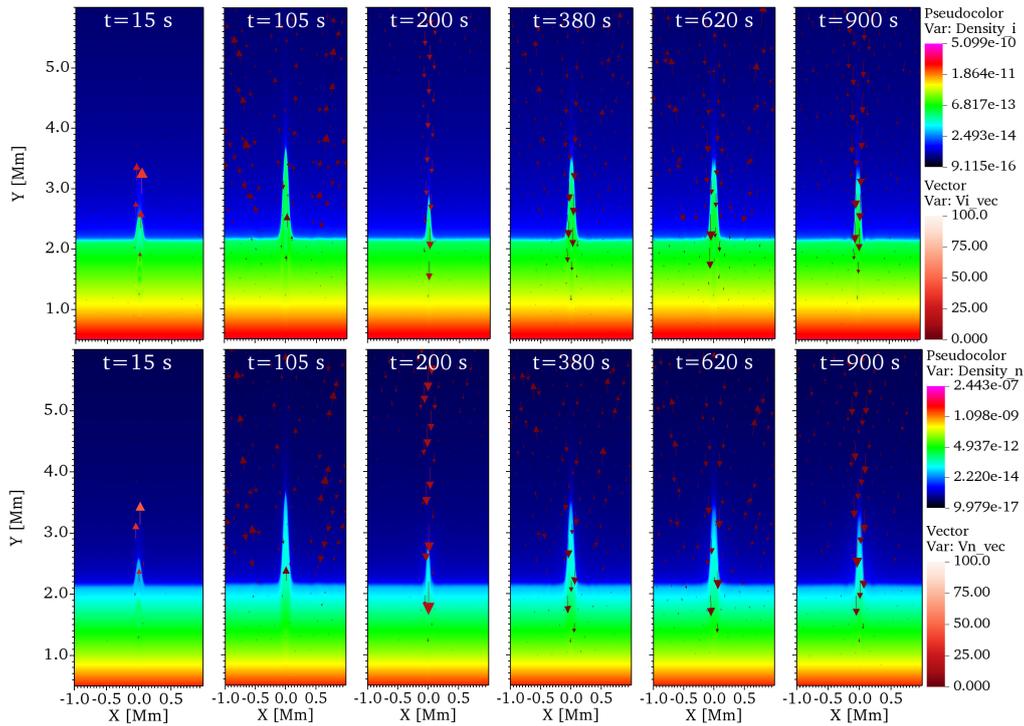
Figure 3. Spatial-temporal variation of density maps in g cm^{-3}, for ions (upper panels) and for neutrals (bottom panels) during launch of cool jets. These jets are triggered by implementing the non-linear transverse pulse (V_z) mimicking Alfvén pules and implemented in the chromosphere at y=1.5 Mm. This pulse produces initially field-aligned perturbations followed by recurrent magnetoacoustic shocks. These shocks create collimated mass transports as cool jets. The red arrows depict the velocity vectors in km s^{-1}, which are overlaid on each density map for ions (upper panels) and neutrals (bottom panels). These velocity vectors shows the upward and downward propagation of jet's plasma in the model solar atmosphere.

As the cooler chromospheric material has a lower ionisation degree than the corona, the ionisation fraction is higher as a result of the spicule. As we do not have ionisation/recombination in the model, which could be heavily active here, our model suffers a drawback in the present simulation in this particular context. We take a slit along the cool jets (in the ions and neutrals maps as demonstrated in the top panels of Fig. 4) to examine their formation and kinematical properties. We follow these spicular jets by clicking on the path coordinates from 2.0 Mm up to 6.0 Mm, and make the distance-time diagrams in log $\rho_{i,n}$ (see the lower panels of Fig 4). The distance-time maps of the magnitude of the Alfvén pulse (V_z), as well as (V_y) in ions and neutrals are calculated along the same chosen slit and displayed in Fig. 5 top and middle panels.

This cool jet is triggered by the energy transfer from Alfvén pulse (cf., Fig. 5, top panel) into the field-aligned perturbation in non-linear regime of two-fluid system. In the 2.5-D two-fluid simulation, this energy transfer initially occurs from applied transverse perturbation into the field-aligned perturbation through ponderomotive force. Later on, this filed-aligned perturbations generate the magnetoacoustic shocks (Fig. 5, middle panel). Some small differences can be seen on profiles $V_i(y)$ and $V_n(y)$, but it is not any significant difference (see middle/bottom-left and middle/bottom-right panels in Fig. 5). These shocks are followed by the cool plasma forming the spicular jets [50,82,83]. These jets are propelled along the magnetic field lines below the shocks in the solar atmosphere. The ponderomotive force is evolved in two-fluid system which is responsible as an initial triggering mechanism for the origin of jets rising and falling on the same path (Fig. 4, bottom panel, Fig. 5, first and second rows) which
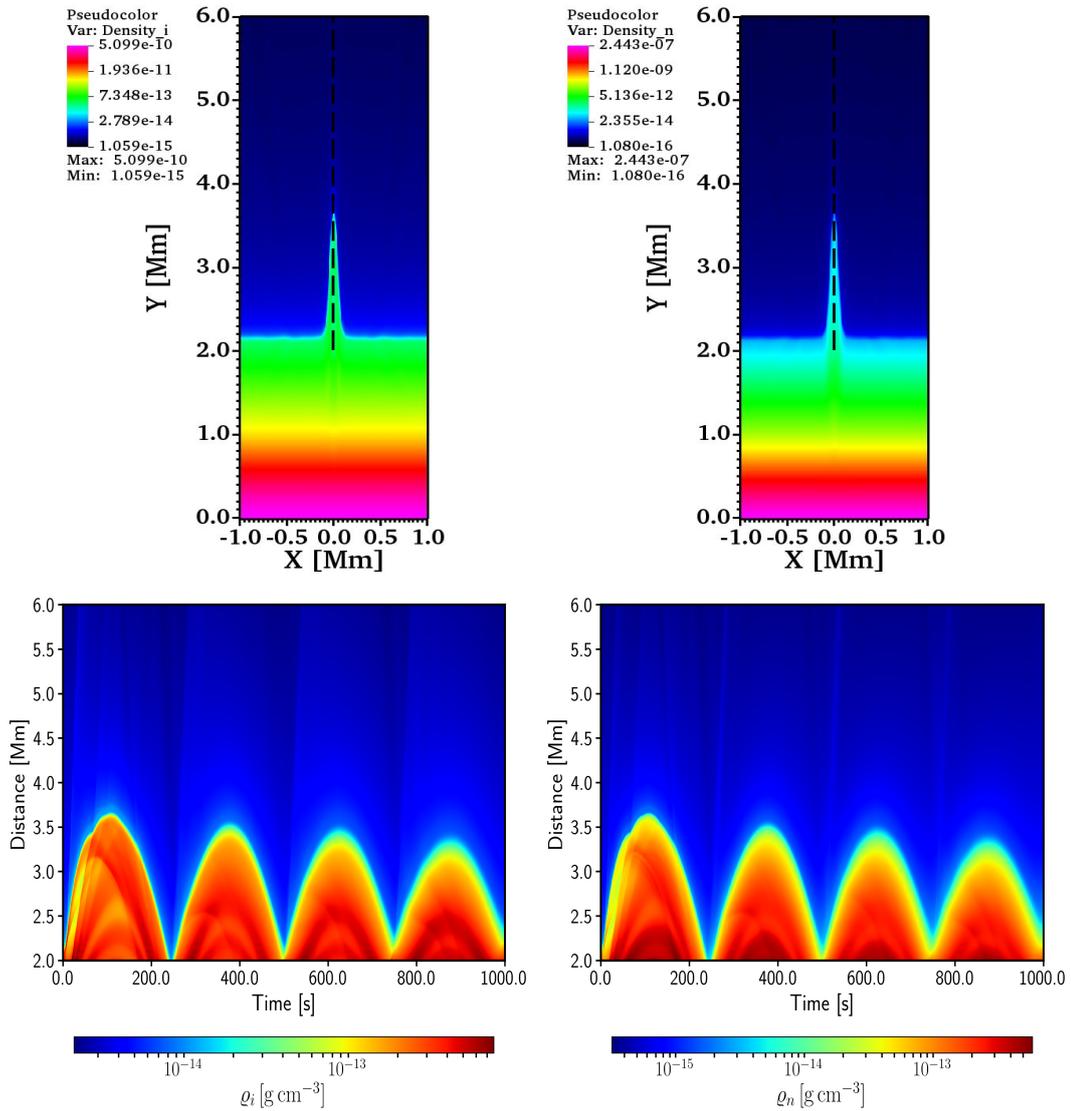
Figure 4. The maps of the mass density (ρ) of ion and neutrals are shown along with the spicular jet in the top panels. The black-dotted slits from 2 to 6 Mm are overlaid on the jet's path along which the distance-time maps are derived and shown in the bottom panels. These maps reveal a recurrent pattern of spicular jets exhibiting quasi-periodic rise and fall in the model solar atmosphere.

is commonly observed in the chromosphere (Figs. 4, 9) [1,6]. The initial pulse in the transversal component of ion and neutral velocity excites in a while perturbations in B_z. The ponderomotive force results from the vertical component of magnetic pressure gradient implied by B_z. As a result of this force, in a low plasma beta region, essentially vertical ion flow, V_{iy}, is generated and the ion-neutral drag, $V_{iy} - V_{ny}$, becomes increased, as neutrals are not directly affected by magnetic field. These neutrals acquire some momentum from ions until their velocities potentially equalize. As a consequence of the drag, some kinetic energy is thermalized leading to temperature increase, and waves become damped, leading to the reduction of the ponderomotive force. Once the first spicule is triggered under this mechanism, then follow-up jets are the response of downflowing spicular plasma due to an imbalance between the pressure gradient and gravity,
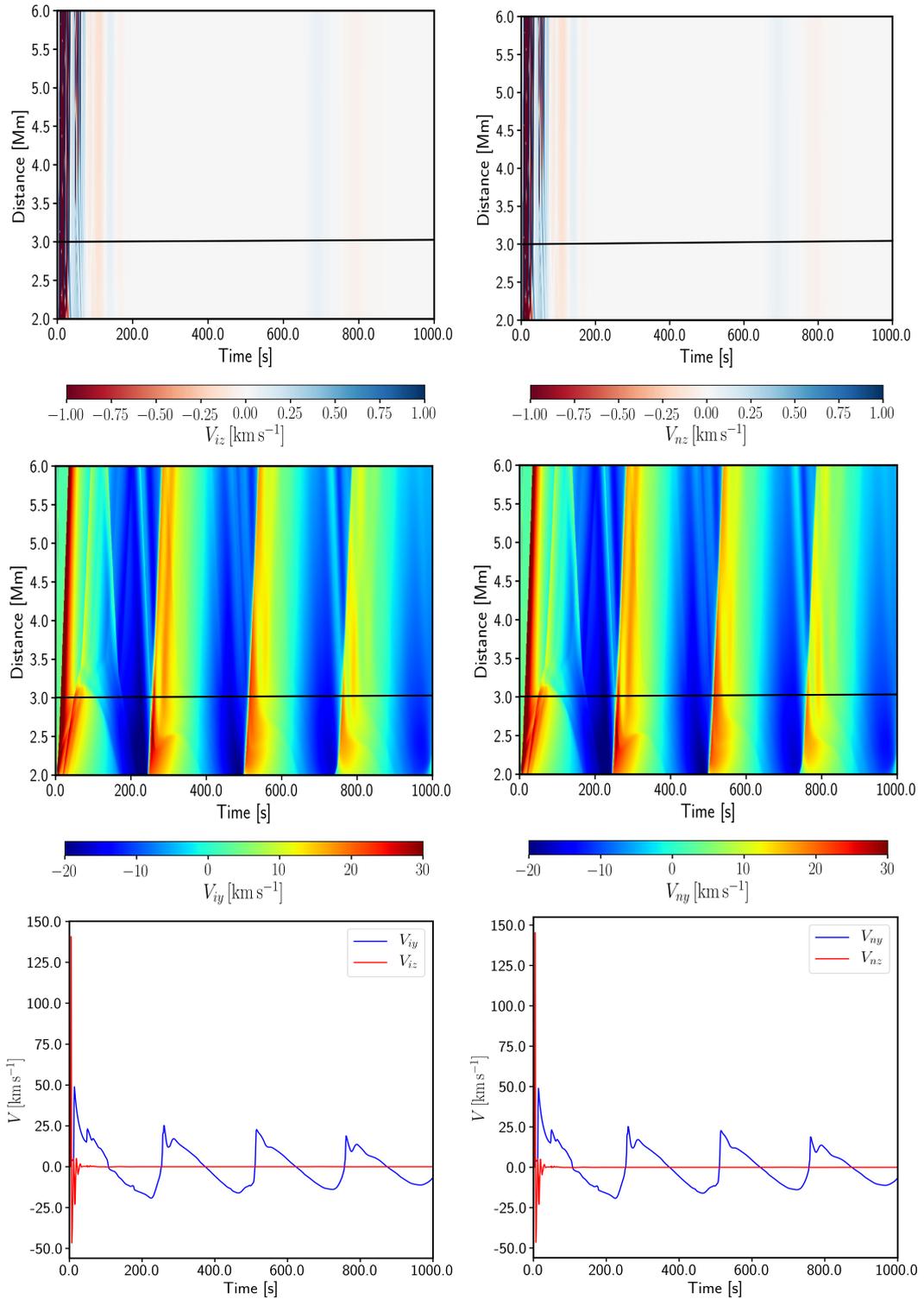
Figure 5. The distance-time maps of the strength of transverse pulse *akin* to the Alfvén pulse (V_z), the vertical field aligned velocity (V_y) in ions and neutrals are estimated along the chosen slit (cf., Fig. 4, top-panel). The temporal evolution of V_{iz}, V_{nz} (red curve) and V_{iy}, V_{ny} (blue curve) along the horizontal black slit taken at y=3.0 Mm (cf., top and middle panels) are shown in the bottom panels. The red curves depict the magnitude of applied Alfvén pulse and blue curves indicate the signature of shock propagating above the spicular jets.

as well as rebound shocks. The transport of the energy from Alfvén pulse to the field aligned perturbations due to ponderomotive force is considered as an initial trigger mechanism. Such physical phenomenon was firstly proposed by Hollweg [50] in 1-D MHD model, who found that the transverse perturbation can produce pure Alfvén pulses above solar photosphere hat may couple with magnetoacoustic shocks/wave to launch spicules.

The similar physical process is modelled and show-cased by [6] in MHD simulations in the ideal plasma. In the present work, we study the effect of ion–neutral collisions and thermal conduction in the formation of cool jets in two-fluid regime, in addition to the non-linear transverse perturbation that trigger them. We adopt a two-fluid model to describe the partially ionized plasma, where ions and neutrals interact through collisions. The degree of ionization varies from 0.1% in the lower chromosphere to 10% in the upper chromosphere, making the ion–neutral collisions significant for the plasma dynamics. The collisions result in friction and momentum transfer between the two fluids, which modify the propagation and damping of magnetoacoustic shocks/waves. These shocks/waves can heat the localized chromosphere by converting their energy into thermal energy, but they can also be attenuated by the collisions and lose their efficiency. The attenuation of the shocks/waves produces additional heating in the localized region of the chromosphere, which plays a significant role in the formation of spicular jet.

In addition, we include the effect of thermal conduction for both ions and neutrals in the model solar atmosphere, which may generically results in some energy transport towards the solar chromosphere, thus causing energy re-distribution during the propagation of these cool jets. However, this causes some background plasma upflows in the model solar atmosphere that enables more increased kinetic motions of the transition region counterpart of the spicular jets [7]. In the present model, thermal conduction may also create the damping of magnetoacoustic shocks/waves [7]. Therefore, the ion–neutral collisions and thermal conduction may have a substantial impact on the formation, triggering/evolution of chromospheric cool jets by influencing their generation, propagation, dissipation, and thermal properties. The detailed analyses of these candidates on the physical properties of cool jets will be the subject of future study.

We perform a wavelet analysis (Fig. 6) on the time-series of estimated mass flux (ρv) in ions and neutrals as collected in the overlying corona at y=3 Mm along the path where spicular jets rise and fall (see Fig. 6, left column, first and second row) [84]. The temporal variation of the mass flux (left-column), wavelet spectra (middle-panel) showing the localized powers in Fourier and time-period space in 2-D space, and global power spectra (right-column; the averaged power over the total time duration for each Fourier period) are shown in Fig. 6 for ions (top-row) and neutrals (bottom-row). By making use of the wavelet analysis tool, the search for the significant oscillatory periods in the given time-series is performed by a time-localized Morlet function that is continuous in both frequency-domain and time [84]. The wavelet is convolved with the time series (here mass flux of ions/neutrals vs time) to estimate the contributions of the frequencies present in it that resembles accurately with the sinusoidal part by varying scale of the wavelet function. This method deduce the power spectrum of the oscillatory patterns present in the signal (see Fig. 6). Here, we use the wavelet tool to estimate the significant periodicity of the quasi-periodic rise and fall of the mass flux associated with spicular jets. The mass motions have been calculated with periodicity of $\simeq 4.41$ min for ions and $\simeq 4.05$ min for neutrals with a > 95 % significance level (Fig. 6). Therefore, the mass flux exhibits a quasi-periodic rise and fall of the plasma in the shape of recurrent cool jets with a typical time scale of $\simeq 4.0$ min.

4. Discussion and Conclusions

In the present scientific work, we performed a 2.5-D numerical simulation in two-fluid system (for ions and neutrals) in the presence of thermal conduction and ion-neutral collision to model the triggering of spicular jets caused by Alfvén pulse. These jets show the quasi-periodic rise and fall at a typical $\simeq 4.0$ min time-scale. The present study provides a numerical modelling of
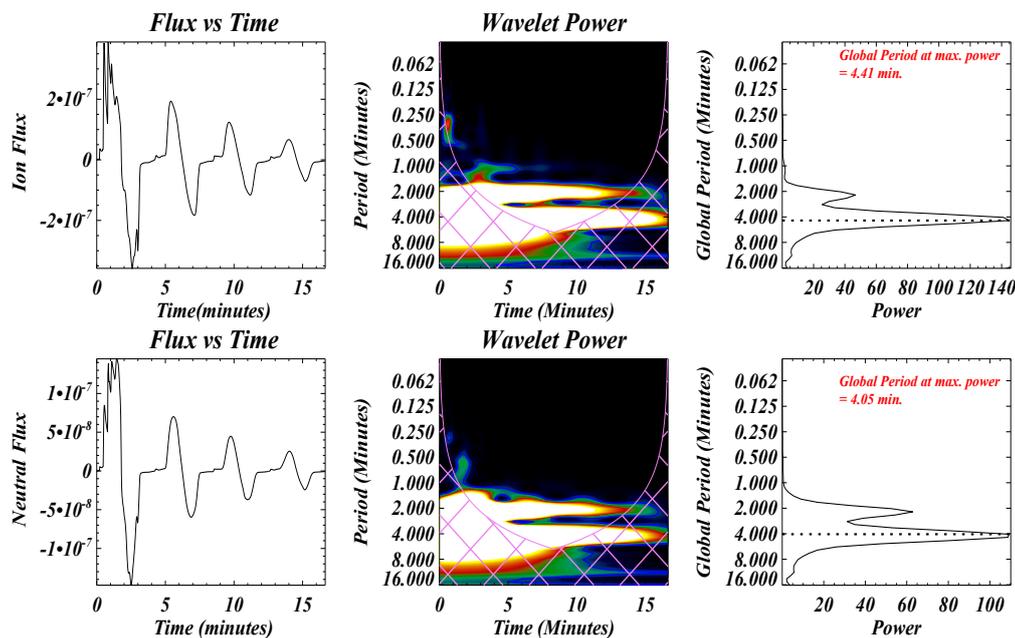
Figure 6. The power spectral analyses using wavelet tool is performed on the temporal variation of the mass flux launched by jets for ions and neutrals. The ion and neutral mass fluxes are estimated at 3.0 Mm height just above the TR in the path of spicular jet as a function of time.

the formation, kinematics, and mass transport due to evolved cool jets. The results show that transverse velocity pulse can produce the strong field-aligned magnetoacoustic perturbations in the solar chromosphere, causing shocks in the stratified overlying atmosphere. This energy exchange can occur in non-linear regime when transverse Alfvén-like perturbation is dissipated and the field-aligned motion due to ponderomotive force is originated [82,85]. Furthermore, these field-aligned perturbations generate the shocks which create lower pressure regions, and drive rise and fall of cool spicular jets quasi-periodically (Fig. 4, bottom panel) to transfer mass into the localized lower corona (Fig. 6). In the present model, we notice that the ion-neutral collisions and thermal conduction may work in the formation of jet and their kinematics. If we exclude these two physical effects from the two fluid simulations, the appropriate height of the jet is not achieved. The jet attains a reasonable height around 4.0 Mm in this two-fluid simulation in the presence of the thermal conduction and ion-neutral collision. However, it should be noted that the driver might have been too strong and further work needs to be done. In the ideal MHD simulations done by [6], the cool spicular jets were even attaining suitable height without implementing the dissipative agents like thermal conduction, etc. The presence of non-ideal, two-fluid plasma in the chromosphere is a more realistic physical configuration of the plasma. In such a plasma configuration, the cool spicule like jets are formed during energy re-distribution due to thermal conduction and the presence of ion-neutral collision as seen in the present simulation. Most likely ion-neutral collision dissipate the part of the energy of wave, thus leading to the reduction of the ponderomotive force, even the amplitude of the Alfvén pulse was strong initially. Therefore, this force does not lead effective field-aligned perturbations likewise in ideal MHD, and does not intend to launch the spicular like jets to the maximum height until the thermal conduction re-distribute the energy and heating generated upflows support the upward motion of the chromospheric plasma together.

We extend and provided new insights on one previous MHD model given by [6] regarding the formation of spicule-like cool jets by adding thermal conduction and ion-neutral collision effects in two-fluid regime. The previous work is performed in 2.5-D simulation in ideal MHD by implementing multiple Alfvén pulses at the solar chromosphere [6]. In that model, randomly generated multiple Alfvén pulses of magnitude between 50-90 Km s^{-1} were applied in the solar chromosphere between 1.5-2.0 Mm. It was demonstrated that the Alfvén pulses generate field-aligned magnetoacoustic perturbations that evolve into shocks, which drive spicule-like mass motions. This mechanism was first proposed by Hollweg [50] in 1-D MHD model, who argued that the transverse perturbation can produce pure Alfvén pulses that may couple with magnetoacoustic shocks/wave responsible for the generation of spicule-like jets.

We performed the similar simulation set-up as reported by [6], however, in two-fluid regime of the solar plasma by also invoking the effects of ion-neutral collisions and thermal conductivity. Our previous numerical modeling by Singh et al. [6] describe the generation of spicule-like cool jets in a similar fashion using ideal and single fluid, 2.5 D MHD. Therefore, our aim here is to just show-case that physical model of the cool jets under more realistic physical conditions, i.e., two fluid regimes including thermal condition and ion-neutral collisions. We do not focus on the parametric study in the present case. Its interesting to note that in the presence of the more appropriate physical conditions of non-ideal partially ionized plasma the spicular jets attain suitable height and appear as a thin plasma column rising and falling quasi-periodically as seen in various observations. When we switched on the thermal conductivity the re-distribution of energy and the damping of waves lead to the formation of these spicule-like cool jets. We assert finally that to understand the exact physics of cool chromosperic jets and their formation, the two-fluid simulations with ion-neutral collision and thermal conductivity may be taken into account in numerical models. Additional physical processes, such as radiative transfer, radiative cooling, radiative transport, ionization, recombination, and heating terms, should be incorporated into future models. These additions will enhance the comprehensiveness and accuracy of the simulations [86,87]. MHD may also be an appropriate formalism but it rules-out neutrals that are present in the lower solar atmosphere and might be at work there in formation of spicular jets.

A. Data Availability

The numerical simulation data that underpins this research is accessible at Dryad (https://doi.org/10.) 1/dryad.jm63xsjjs) and can be shared with the corresponding author upon reasonable request.

References

1. De Pontieu B, Erdélyi R, James SP.
   Solar chromospheric spicules from the leakage of photospheric oscillations and flows.
   Nature. 2004 Jul;430(6999):536-9.
2. Tian H, DeLuca EE, Cranmer SR, De Pontieu B, Peter H, Martínez-Sykora J, et al.
   Prevalence of small-scale jets from the networks of the solar transition region and chromosphere.
   Science. 2014 Oct;346(6207):1255711.
3. Martínez-Sykora J, De Pontieu B, Hansteen VH, Rouppe van der Voort L, Carlsson M, Pereira TMD.
   On the generation of solar spicules and Alfvénic waves.
   Science. 2017 Jun;356(6344):1269-72.
4. Singh B, Sharma K, Srivastava AK.
   On modelling the kinematics and evolutionary properties of pressure-pulse-driven impulsive solar jets.
   Annales Geophysicae. 2019 Sep;37(5):891-902.
5. González-Avilés JJ, Guzmán FS, Fedun V, Verth G.
   Spicule Jets in the Solar Atmosphere Modeled with Resistive MHD and Thermal Conduction.
   The Astrophysical Journal. 2020 Jul;897(2):153.
6. Singh B, Srivastava AK, Sharma K, Mishra SK, Dwivedi BN.
   Quasi-periodic spicule-like cool jets driven by Alfvén pulses.
   Monthly Notices of Royal Astronomical Society. 2022 Apr;511(3):4134-46.
7. Srivastava AK, Singh B, Murawski K, Chen Y, Sharma K, Yuan D, et al.
   Impulsive origin of solar spicule-like jets.
   European Physical Journal Plus. 2023 Mar;138(3):209.
8. Mishra SK, Sangal K, Kayshap P, Jelínek P, Srivastava AK, Rajaguru SP.
   Origin of Quasi-periodic Pulsation at the Base of a Kink-unstable Jet.
   Astrophysical Journal. 2023 Mar;945(2):113.
9. Hansteen VH, Hara H, De Pontieu B, Carlsson M.
   On Redshifts and Blueshifts in the Transition Region and Corona.
   Astrophysical Journal. 2010 Aug;718(2):1070-8.
10. Antolin P, Schmit D, Pereira TMD, De Pontieu B, De Moortel I.
    Transverse Wave Induced Kelvin-Helmholtz Rolls in Spicules.
    Astrophysical Journal. 2018 Mar;856(1):44.
11. Martínez-Sykora J, Leenaarts J, De Pontieu B, Nóbrega-Siverio D, Hansteen VH, Carlsson M, et al.
    Ion-neutral Interactions and Nonequilibrium Ionization in the Solar Chromosphere.
    Astrophysical Journal. 2020 Feb;889(2):95.
12. Mishra SK, Singh B, Srivastava AK, Kayshap P, Dwivedi BN.
    Evolution of Kelvin-Helmholtz Instability in the Fan-spine Topology.
    The Astrophysical Journal. 2021 Dec;923(1):72.
13. Srivastava AK, Singh B.
    Numerical Simulations of the Decaying Transverse Oscillations in the Cool Jet.
    Physics. 2023 Jun;5(3):655-71.
14. Hansteen VH, De Pontieu B, Rouppe van der Voort L, van Noort M, Carlsson M.
    Dynamic Fibrils Are Driven by Magnetoacoustic Shocks.
    Astrophysical Journal Letters. 2006 Aug;647(1):L73-6.
15. De Pontieu B, Hansteen VH, Rouppe van der Voort L, van Noort M, Carlsson M.
    High-Resolution Observations and Modeling of Dynamic Fibrils.
    The Astrophysical Journal. 2007 Jan;655(1):624-41.
16. Rouppe van der Voort L, Leenaarts J, de Pontieu B, Carlsson M, Vissers G.

On-disk Counterparts of Type II Spicules in the Ca II 854.2 nm and Hα Lines.
The Astrophysical Journal. 2009 Nov;705(1):272-84.

17. Sterling AC, Harra LK, Moore RL.
Fibrillar Chromospheric Spicule-like Counterparts to an Extreme-ultraviolet and Soft X-ray Blowout Coronal Jet.
The Astrophysical Journal. 2010 Oct;722(2):1644-53.

18. De Pontieu B, McIntosh SW, Carlsson M, Hansteen VH, Tarbell TD, Boerner P, et al.
The Origins of Hot Plasma in the Solar Corona.
Science. 2011 Jan;331(6013):55.

19. Wedemeyer-Böhm S, Scullion E, Steiner O, Rouppe van der Voort L, de La Cruz Rodriguez J, Fedun V, et al.
Magnetic tornadoes as energy channels into the solar corona.
Nature. 2012 Jun;486(7404):505-8.

20. Shetye J, Doyle JG, Scullion E, Nelson CJ, Kuridze D, Henriques V, et al.
High-cadence observations of spicular-type events on the Sun.
Astronomy & Astrophysics. 2016 May;589:A3.

21. Samanta T, Tian H, Yurchyshyn V, Peter H, Cao W, Sterling A, et al.
Generation of solar spicules and subsequent atmospheric heating.
Science. 2019 Nov;366(6467):890-4.

22. Srivastava AK, Murawski K, Kuźma B, Wójcik DP, Zaqarashvili TV, Stangalini M, et al.
Confined pseudo-shocks as an energy source for the active solar corona.
Nature Astronomy. 2018 Oct;2:951-6.

23. Pasachoff JM, Jacobson WA, Sterling AC.
Limb Spicules from the Ground and from Space.
Solar Physics. 2009 Nov;260(1):59-82.

24. Pereira TMD, Carlsson M, De Pontieu B, Hansteen V.
The Formation of IRIS Diagnostics. IV. The Mg II Triplet Lines as a New Diagnostic for Lower Chromospheric Heating.
Astrophysical Journal. 2015 Jun;806(1):14.

25. Takasao S, Isobe H, Shibata K.
Numerical Simulations of Solar Chromospheric Jets Associated with Emerging Flux.
Publications of the Astronomical Society of Japan. 2013 Jun;65:62.

26. Tsiropoula G, Tziotziou K, Kontogiannis I, Madjarska MS, Doyle JG, Suematsu Y.
Solar Fine-Scale Structures. I. Spicules and Other Small-Scale, Jet-Like Events at the Chromospheric Level: Observations and Physical Parameters.
Space Sci Rev. 2012 Sep;169(1-4):181-244.

27. Murawski K, Srivastava AK, Zaqarashvili TV.
Numerical simulations of solar macrospicules.
Astronomy & Astrophysics. 2011 Nov;535:A58.

28. Adams M, Sterling AC, Moore RL, Gary GA.
A Small-scale Eruption Leading to a Blowout Macrospicule Jet in an On-disk Coronal Hole.
Astrophysical Journal. 2014 Mar;783(1):11.

29. Loboda IP, Bogachev SA.
What is a Macrospicule?
Astrophysical Journal. 2019 Feb;871(2):230.

30. González-Avilés JJ, Murawski K, Srivastava AK, Zaqarashvili TV, González-Esparza JA.
Numerical simulations of macrospicule jets under energy imbalance conditions in the solar atmosphere.
Monthly Notices of Royal Astronomical Society. 2021 Jul;505(1):50-64.

31. Duan Y, Shen Y, Chen H, Tang Z, Zhou C, Zhou X, et al.
Macrospicules and Their Connection to Magnetic Reconnection in the Lower Solar Atmosphere.
Astrophysical Journal Letters. 2023 Jan;942(1):L22.

32. Pereira TMD, De Pontieu B, Carlsson M, Hansteen V, Tarbell TD, Lemen J, et al.
An Interface Region Imaging Spectrograph First View on Solar Spicules.
The Astrophysical Journall. 2014 Sep;792(1):L15.

33. Chen Y, Tian H, Huang Z, Peter H, Samanta T.
Investigating the Transition Region Explosive Events and Their Relationship to Network Jets.

18

royalsocietypublishing.org/journal/rsta   Phil. Trans. R. Soc. A 0000000

The Astrophysical Journal. 2019 Mar;873(1):79.

34. Kayshap P, Murawski K, Srivastava AK, Dwivedi BN.
Rotating network jets in the quiet Sun as observed by IRIS.
Astronomy & Astrophysics. 2018 Aug;616:A99.

35. Pariat E, Dalmasse K, DeVore CR, Antiochos SK, Karpen JT.
Model for straight and helical solar jets. I. Parametric studies of the magnetic field geometry.
Astronomy & Astrophysics. 2015 Jan;573:A130.

36. Iijima H, Yokoyama T.
A Three-dimensional Magnetohydrodynamic Simulation of the Formation of Solar Chromospheric Jets with Twisted Magnetic Field Lines.
The Astrophysical Journal. 2017 Oct;848(1):38.

37. Uddin W, Schmieder B, Chandra R, Srivastava AK, Kumar P, Bisht S.
Observations of Multiple Surges Associated with Magnetic Activities in AR 10484 on 2003 October 25.
Astrophysical Journal. 2012 Jun;752(1):70.

38. Nóbrega-Siverio D, Moreno-Insertis F, Martínez-Sykora J.
The Cool Surge Following Flux Emergence in a Radiation-MHD Experiment.
Astrophysical Journal. 2016 May;822(1):18.

39. Nóbrega-Siverio D, Martínez-Sykora J, Moreno-Insertis F, Rouppe van der Voort L.
Surges and Si IV Bursts in the Solar Atmosphere: Understanding IRIS and SST Observations through RMHD Experiments.
Astrophysical Journal. 2017 Dec;850(2):153.

40. Joshi R, Chandra R, Schmieder B, Moreno-Insertis F, Aulanier G, Nóbrega-Siverio D, et al.
Case study of multi-temperature coronal jets for emerging flux MHD models.
Astronomy & Astrophysics. 2020 Jul;639:A22.

41. Sterling AC.
Solar Spicules: A Review of Recent Models and Targets for Future Observations - (Invited Review).
Solar Physics. 2000 Sep;196(1):79-111.

42. Schmieder B, Shibata K, van Driel-Gesztelyi L, Freeland S.
Hα surges and associated Soft X-ray loops.
Solar Physics. 1995 Feb;156(2):245-64.

43. Ding JY, Madjarska MS, Doyle JG, Lu QM, Vanninathan K, Huang Z.
Magnetic reconnection resulting from flux emergence: implications for jet formation in the lower solar atmosphere?
Astronomy & Astrophysics. 2011 Nov;535:A95.

44. Shibata K, Nishikawa T, Kitai R, Suematsu Y.
Numerical Hydrodynamics of the Jet Phenomena in the Solar Atmosphere - Part Two - Surges.
Solar Physics. 1982 Apr;77(1-2):121-51.

45. Nishizuka N, Shimizu M, Nakamura T, Otsuji K, Okamoto TJ, Katsukawa Y, et al.
Giant Chromospheric Anemone Jet Observed with Hinode and Comparison with Magnetohydrodynamic Simulations: Evidence of Propagating Alfvén Waves and Magnetic Reconnection.
The Astrophysical Journall. 2008 Aug;683(1):L83.

46. Kayshap P, Srivastava AK, Murawski K, Tripathi D.
Origin of Macrospicule and Jet in Polar Corona by a Small-scale Kinked Flux Tube.
The Astrophysical Journall. 2013 Jun;770(1):L3.

47. Heggland L, De Pontieu B, Hansteen VH.
Numerical Simulations of Shock Wave-driven Chromospheric Jets.
The Astrophysical Journal. 2007 Sep;666(2):1277-83.

48. Murawski K, Zaqarashvili TV.
Numerical simulations of spicule formation in the solar atmosphere.
Astronomy & Astrophysics. 2010 Sep;519:A8.

49. Martínez-Sykora J, Hansteen V, Moreno-Insertis F.
On the Origin of the Type II Spicules: Dynamic Three-dimensional MHD Simulations.
The Astrophysical Journal. 2011 Jul;736(1):9.

50. Hollweg JV.
On the origin of solar spicules.

The Astrophysical Journal. 1982 Jun;257:345-53.

51. Kudoh T, Shibata K.
Alfvén Wave Model of Spicules and Coronal Heating.
The Astrophysical Journal. 1999 Mar;514(1):493-505.

52. Kuźma B, Murawski K, Zaqarashvili TV, Konkol P, Mignone A.
Numerical simulations of solar spicules: Adiabatic and non-adiabatic studies.
Astronomy & Astrophysics. 2017 Jan;597:A133.

53. Mackenzie Dover F, Sharma R, Erdélyi R.
Magnetohydrodynamic Simulations of Spicular Jet Propagation Applied to Lower Solar
Atmosphere Model.
The Astrophysical Journal. 2021 May;913(1):19.

54. Ballester JL, Alexeev I, Collados M, Downes T, Pfaff RF, Gilbert H, et al.
Partially Ionized Plasmas in Astrophysics.
Space Science Reviews. 2018 Mar;214(2):58.

55. Wójcik D, Kuźma B, Murawski K, Musielak ZE.
Wave heating of the solar atmosphere without shocks.
Astronomy & Astrophysics. 2020 Mar;635:A28.

56. Kuźma B, Murawski K, Poedts S.
3D numerical simulations of propagating two-fluid, torsional Alfvén waves and heating of a
partially ionized solar chromosphere.
Monthly Notices of Royal Astronomical Society. 2021 Sep;506(1):989-96.

57. James SP, Erdélyi R, De Pontieu B.
Can ion-neutral damping help to form spicules?
Astronomy & Astrophysics. 2003 Aug;406:715-24.

58. Khomenko E, Collados M.
Heating of the Magnetized Solar Chromosphere by Partial Ionization Effects.
The Astrophysical Journal. 2012 Mar;747(2):87.

59. Soler R, Carbonell M, Ballester JL.
Magnetoacoustic Waves in a Partially Ionized Two-fluid Plasma.
The Astrophysical Journals. 2013 Nov;209(1):16.

60. Khomenko E.
On the effects of ion-neutral interactions in solar plasmas.
Plasma Physics and Controlled Fusion. 2017 Jan;59(1):014038.

61. Kuźma B, Murawski K, Kayshap P, Wójcik D, Srivastava AK, Dwivedi BN.
Two-fluid Numerical Simulations of Solar Spicules.
The Astrophysical Journal. 2017 Nov;849(2):78.

62. Popescu Braileanu B, Lukin VS, Khomenko E, de Vicente Á.
Two-fluid simulations of waves in the solar chromosphere. II. Propagation and damping of
fast magneto-acoustic waves and shocks.
Astronomy & Astrophysics. 2019 Oct;630:A79.

63. Zaqarashvili TV, Khodachenko ML, Rucker HO.
Damping of Alfvén waves in solar partially ionized plasmas: effect of neutral helium in multi-
fluid approach.
Astronomy & Astrophysics. 2011 Oct;534:A93.

64. Sakai JI, Smith PD, Futagami Y.
Two-Fluid Simulations of Chromospheric Heating by Alfvén Wave Pulses and Slow
Magnetosonic Wave Pulses.
In: Sekii T, Watanabe T, Sakurai T, editors. Hinode-3: The 3rd Hinode Science Meeting. vol.
454 of Astronomical Society of the Pacific Conference Series; 2012. p. 129.

65. Meier ET, Shumlak U.
A general nonlinear fluid model for reacting plasma-neutral mixtures.
Physics of Plasmas. 2012 Jul;19(7):072508.

66. Leake JE, DeVore CR, Thayer JP, Burns AG, Crowley G, Gilbert HR, et al.
Ionized Plasma and Neutral Gas Coupling in the Sun's Chromosphere and Earth's
Ionosphere/Thermosphere.
Space Sci Rev. 2014 Nov;184(1-4):107-72.

67. Oliver R, Soler R, Terradas J, Zaqarashvili TV.
Dynamics of Coronal Rain and Descending Plasma Blobs in Solar Prominences. II. Partially
Ionized Case.

Astrophysical Journal. 2016 Feb;818(2):128.

68. Maneva YG, Alvarez Laguna A, Lani A, Poedts S.
Multi-fluid Modeling of Magnetosonic Wave Propagation in the Solar Chromosphere: Effects of Impact Ionization and Radiative Recombination.
Astrophysical Journal. 2017 Feb;836(2):197.

69. Popescu Braileanu B, Lukin VS, Khomenko E, de Vicente Á.
Two-fluid simulations of waves in the solar chromosphere. I. Numerical code verification.
Astronomy & Astrophysics. 2019 Jul;627:A25.

70. Murawski K, Musielak ZE, Poedts S, Srivastava AK, Kadowaki L.
Two-fluid numerical model of chromospheric heating and plasma outflows in a quiet-Sun.
Astrophysics and Space Science. 2022 Nov;367(11):111.

71. Braginskii SI.
Transport Processes in a Plasma.
Reviews of Plasma Physics. 1965 Jan;1:205.

72. Zaqarashvili TV, Khodachenko ML, Rucker HO.
Magnetohydrodynamic waves in solar partially ionized plasmas: two-fluid approach.
Astronomy & Astrophysics. 2011 May;529:A82.

73. Vranjes J, Krstic PS.
Collisions, magnetization, and transport coefficients in the lower solar atmosphere.
Astronomy & Astrophysics. 2013 Jun;554:A22.

74. Cranmer SR, van Ballegooijen AA, Edgar RJ.
Self-consistent Coronal Heating and Solar Wind Acceleration from Anisotropic Magnetohydrodynamic Turbulence.
The Astrophysical Journals. 2007 Aug;171(2):520-51.

75. Spitzer L.
Physics of Fully Ionized Gases; 1962.

76. Honda M.
Coulomb Logarithm Formulae for Collisions between Species with Different Temperatures.
Japanese Journal of Applied Physics. 2013 Oct;52(10R):108002.

77. Avrett EH, Loeser R.
Models of the Solar Chromosphere and Transition Region from SUMER and HRTS Observations: Formation of the Extreme-Ultraviolet Spectrum of Hydrogen, Carbon, and Oxygen.
The Astrophysical Journals. 2008 Mar;175(1):229-76.

78. Low BC.
Three-dimensional structures of magnetostatic atmospheres. I - Theory.
The Astrophysical Journal. 1985 Jun;293:31-43.

79. Priest E.
Magnetohydrodynamics of the Sun.
Cambridge University Press; 2014.

80. De Pontieu B, McIntosh SW, Carlsson M, Hansteen VH, Tarbell TD, Schrijver CJ, et al.
Chromospheric Alfvénic Waves Strong Enough to Power the Solar Wind.
Science. 2007 Dec;318(5856):1574.

81. Okamoto TJ, De Pontieu B.
Propagating Waves Along Spicules.
Astrophysical Journal Letters. 2011 Aug;736(2):L24.

82. Verwichte E, Nakariakov VM, Longbottom AW.
On the evolution of a nonlinear Alfvén pulse.
Journal of Plasma Physics. 1999 Aug;62(2):219-32.

83. Thurgood JO, McLaughlin JA.
On Ponderomotive Effects Induced by Alfvén Waves in Inhomogeneous 2.5D MHD Plasmas.
Solar Physics. 2013 Nov;288(1):205-22.

84. Torrence C, Compo GP.
A Practical Guide to Wavelet Analysis.
Bulletin of the American Meteorological Society. 1998 Jan;79(1):61-78.

85. Murawski K, Solov'ev A, Musielak ZE, Srivastava AK, Kraśkiewicz J.
Torsional Alfvén waves in solar magnetic flux tubes of axial symmetry.
Astronomy & Astrophysics. 2015 May;577:A126.

86. Snow B, Druett MK, Hillier A.
    Partially ionized two-fluid shocks with collisional and radiative ionization and recombination
    - multilevel hydrogen model.
    Monthly Notices of the Royal Astronomical Society. 2023 Nov;525(3):4717-34.
87. Zhang F, Poedts S, Lani A, Kuźma B, Murawski K.
    Two-fluid Modeling of Acoustic Wave Propagation in Gravitationally Stratified Isothermal
    Media.
    Astrophysical Journal. 2021 Apr;911(2):119.